Article

Insight into the Mechanisms of Cooperative Self-Assembly: The "Sergeants-and-Soldiers" Principle of Chiral and Achiral C-Symmetrical Discotic Triamides

Maarten M. J. Smulders, Albertus P. H. J. Schenning, and E. W. Meijer

J. Am. Chem. Soc., **2008**, 130 (2), 606-611 • DOI: 10.1021/ja075987k

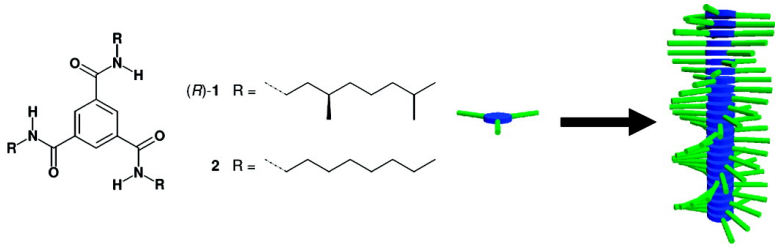

More About This Article

Additional resources and features associated with this article are available within the HTML version:

- Supporting Information
- Links to the 13 articles that cite this article, as of the time of this article download
- Access to high resolution figures
- Links to articles and content related to this article
- Copyright permission to reproduce figures and/or text from this article

View the Full Text HTML

J|A|C|S
ARTICLES
Published on Web 12/15/2007

Insight into the Mechanisms of Cooperative Self-Assembly: The "Sergeants-and-Soldiers" Principle of Chiral and Achiral C_3-Symmetrical Discotic Triamides

Maarten M. J. Smulders, Albertus P. H. J. Schenning,* and E. W. Meijer*

Laboratory of Macromolecular and Organic Chemistry, Eindhoven University of Technology, P.O. Box 415, 5600 MB Eindhoven, The Netherlands

Received August 9, 2007; E-mail: a.p.h.j.schenning@tue.nl; e.w.meijer@tue.nl

Abstract: On the basis of temperature-dependent UV−vis and circular dichroism (CD) spectroscopy measurements, we observed that C_3-symmetrical discotic molecules, chiral (*R*)-**1** and achiral **2**, both self-assemble in a highly cooperative fashion. Chiral (*R*)-**1** shows a higher degree of cooperativity, meaning it requires a larger nucleus before elongation sets in, as compared to achiral **2**. Next to that, we investigated the mechanism of the "sergeants-and-soldiers" principle, where we found that the chiral sergeant (*R*)-**1** strongly amplifies the preference in handedness of the mixed stacks of (*R*)-**1** and **2**. However, the elongation temperature and the degree of cooperativity are linearly dependent on both, at least in the regime above 4% of sergeant in the mixed system. Remarkably, we observed that at room temperature a fast exchange on the second time scale exists between molecules and stacks of sergeant (*R*)-**1** and soldier **2**, and that interconversion between M and P helices is fast at this temperature.

Introduction

Chemical self-assembly offers an attractive approach for the development of complex, supramolecular nanostructures, starting from relatively small and simple molecules. Remarkably, and in contrast to the numerous reports which deal with self-assembled structures, there is only a limited number of papers that deal with the mechanisms of the processes by which these molecules self-assemble. For the rational design and construction of more complex structures, however, it is crucial to unravel the self-assembly mechanisms, as these will determine the noncovalent synthetic routes.[1]

Isodesmic (or equal-*K*) self-assembly[2] has been reported for linear self-assembly of organic molecules[3−10] and is indeed operative in, for example, our supramolecular polymers based on ureido pyrimidinone units.[11] Cooperative self-assembly has been described by a modified isodesmic model[2] in which all, but the first association constant, that is, the dimerization constant, are assumed to be equal.[12−14] This model has its limitation since it assumes that only the first noncovalent assembly step is different from all the other steps. In biochemical systems however, cooperative self-assembly of proteins has been described by a nucleation-growth model,[15−19] which is characterized by the unfavorable formation of nuclei of a critical size, followed by a favorable elongation process.

We have recently used a modified nucleation-growth model, originally developed by Oosawa and Kasai,[16] to describe the cooperative self-assembly of organic π-conjugated molecules into helical fibers.[20] For the temperature-dependent self-assembly of chiral oligo(*p*-phenylenevinylene) derivatives, two temperature regimes could be distinguished: the nucleation and the elongation regime, which were separated by the elongation temperature. Above the elongation temperature, most of the system is in the inactive, nonhelical state (nucleation regime), at the elongation temperature activation occurs, and then below the elongation temperature growth of the chiral aggregate takes place (elongation regime). The activation step is governed by a dimensionless equilibrium constant K_a.

(1) Service, R. F. *Science* **2005**, *309*, 95.
(2) Martin, R. B. *Chem. Rev.* **1996**, *96*, 3043−3064.
(3) Chen, Z.; Stepanenko, V.; Dehm, V.; Prins, P.; Siebbeles, L. D. A.; Seibt, J.; Marquetand, P.; Engel, V.; Würthner, F. *Chem. Eur. J.* **2007**, *13*, 436−449.
(4) Würthner, F.; Thalacker, C.; Diele, S.; Tschierske, C. *Chem. Eur. J.* **2001**, *7*, 2245−2253.
(5) Kastler, M.; Pisula, W.; Wasserfallen, D.; Pakula, T.; Müllen, K. *J. Am. Chem. Soc.* **2005**, *127*, 4286−4296.
(6) Lahiri, S.; Thompson, J. L.; Moore, J. S. *J. Am. Chem. Soc.* **2000**, *122*, 11315−11319.
(7) Stončius, S.; Orentas, E.; Butkus, E.; Öhrström, L.; Wendt, O. F.; Wärnmark, K. *J. Am. Chem. Soc.* **2006**, *128*, 8272−8285.
(8) Tobe, Y.; Utsumi, N.; Kawabata, K.; Nagano, A.; Adachi, K.; Araki, S.; Sonoda, M.; Hirose, K.; Naemura, K. *J. Am. Chem. Soc.* **2002**, *124*, 5350−5364.
(9) van Herrikhuyzen, J.; Syamakumari, A.; Schenning, A. P. H. J.; Meijer, E. W. *J. Am. Chem. Soc.* **2004**, *126*, 10021−10027.
(10) Wang, W.; Han, J. J.; Wang, L. Q.; Li, L. S.; Shaw, W. J.; Li, A. D. Q. *Nano Lett.* **2003**, *3*, 455−458.
(11) Sijbesma, R. P.; Beijer, F. H.; Brunsveld, L.; Folmer, B. J. B.; Hirschberg, J. H. K. K.; Lange, R. F. M.; Lowe, J. K. L.; Meijer, E. W. *Science* **1997**, *278*, 1601−1604.
(12) de Loos, M.; van Esch, J.; Kellogg, R. M.; Feringa, B. L. *Angew. Chem., Int. Ed.* **2001**, *40*, 613−616.
(13) Arnaud, A.; Belleney, J.; Boué, F.; Bouteiller, L.; Carrot, G.; Wintgens, V. *Angew. Chem., Int. Ed.* **2004**, *43*, 1718−1721.
(14) Colombani, O.; Bouteiller, L. *New J. Chem.* **2004**, *28*, 1373−1382.
(15) Klug, A. *Philos. Trans. R. Soc. London, Ser. B* **1999**, *354*, 531−535.
(16) Oosawa, F.; Kasai, M. *J. Mol. Biol.* **1962**, *4*, 10−21.
(17) Krishnan, R.; Lindquist, S. L. *Nature* **2005**, *435*, 765−772.
(18) Knight, J. D.; Hebda, J. A.; Miranker, A. D. *Biochemistry* **2006**, *45*, 9496−9508.
(19) Zhao, D.; Moore, J. S. *Org. Biomol. Chem.* **2003**, *1*, 3471−3491.
(20) Jonkheijm, P.; van der Schoot, P.; Schenning, A. P. H. J.; Meijer, E. W. *Science* **2006**, *313*, 80−83.

 10.1021/ja075987k CCC: $40.75

Scheme 1. Structure of C_3-Symmetrical Chiral Discotic (*R*)-**1** and Its Achiral Analogue **2** (Left) and a Representation of the C_3-Symmetrical Disc Arranged in a Helical Stack (Right)

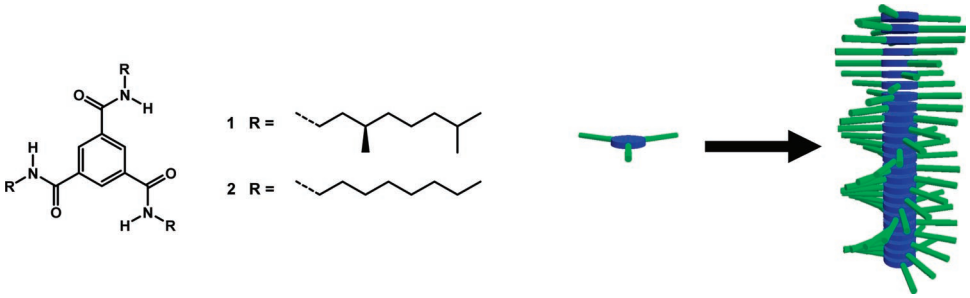

Our model, which is based on temperature-dependent spectroscopic measurements, allows us to characterize the self-assembly processes of any system in detail and not only for the particular π-conjugated oligomer described above. The model will provide information on the degree of cooperativity, the enthalpy release during self-assembly, and the stack growth and length. To explore the generality of cooperative self-assembly, we have now studied with our model the self-assembly mechanisms of C_3-symmetrical trialkylbenzene-1,3,5-tricarboxamides, that is, chiral (*R*)-**1** and achiral **2** (Scheme 1), one of the simplest and most studied building blocks in self-assembly.[21−39] On the basis of temperature-dependent UV−vis and circular dichroism (CD) spectroscopy measurements, we found that discotic molecules (*R*)-**1** and **2**[21,40] both self-assemble in a highly cooperative fashion. Furthermore, to be able to use the modified Oosawa−Kasai model,[41] we have simplified our modeling procedures to fit the temperature-dependent spectroscopy data and made our model generally applicable for researchers active in the field of self-assembly. Finally, we investigated the mechanisms of the "sergeants-and-soldiers" principle,[21] where we observed that the chiral sergeant (*R*)-**1** strongly amplifies the preference in handedness of the mixed stacks of (*R*)-**1** and **2**. Next to that, we found that at room temperature the sergeants-and-soldiers present is fully installed on the time scale of seconds, suggesting there is a rapid exchange between molecules and stacks of sergeant (*R*)-**1** and soldier **2**.

Results

Self-assembly in Solution followed by CD Spectroscopy. The self-assembly of chiral (*R*)-**1** was first investigated with temperature-dependent CD spectroscopy measurements in dilute heptane solution (Figure 1A). Upon cooling the solution, the appearance of a bisignated Cotton effect with a positive value at higher wavelength (223 nm) could be observed, which is in agreement with earlier reports and indicative of the formation of right-handed chiral helical columnar aggregates.[21,42] To study the self-assembly of (*R*)-**1** in helical aggregates in detail, we monitored the molar ellipticity at 223 nm, while cooling solutions with different concentrations from 363 K (where (*R*)-**1** is in the molecular dissolved state, vide infra) to 293 K. In this way, the appearance of a CD signal could be directly related to the formation of helical aggregates (Figure 1B). To ensure that self-assembly was under thermodynamic control, a slow cooling rate of -1 K·min^{-1} was applied. For this cooling rate no hysteresis in the molar ellipticity was observed when heating the solution again to 363 K. In addition, slower cooling rates did not affect the melting curves. Also during all CD measurements no linear dichroism as a result of unintended convective flow was observed.[43]

The melting curves obtained for (*R*)-**1** (Figure 1B) are clearly not sigmoidal, which is indicative of a cooperative self-assembly process. To analyze the temperature-dependent data, we applied the nucleation−elongation model, which describes the cooperative assembly of molecules in linear, one-dimensional aggregates.[41] To model the data we simplified our modeling procedures.[44]

In the elongation regime the fraction of aggregated molecules, ϕ_n, is given by the following equation:[45]

$$\phi_n = \phi_{SAT}\left(1 - \exp\left[\frac{-h_e}{RT_e^2}(T - T_e)\right]\right) \qquad (1)$$

(21) Brunsveld, L.; Schenning, A. P. H. J.; Broeren, M. A. C.; Janssen, H. M.; Vekemans, J. A. J. M.; Meijer, E. W. *Chem. Lett.* **2000**, 292−293.
(22) Matsunaga, Y.; Miyajima, N.; Nakayasu, Y.; Sakai, S.; Yonenaga, M. *Bull. Chem. Soc. Jpn.* **1988**, *61*, 207−210.
(23) Lightfoot, M. P.; Mair, F. S.; Pritchard, R. G.; Warren, J. E. *Chem. Commun.* **1999**, 1945−1946.
(24) van Gorp, J. J.; Vekemans, J. A. J. M.; Meijer, E. W. *J. Am. Chem. Soc.* **2002**, *124*, 14759−14769.
(25) Yasuda, Y.; Iishi, E.; Inada, H.; Shirota, Y. *Chem. Lett.* **1996**, 575−576.
(26) Wilson, A. J.; Masuda, M.; Sijbesma, R. P.; Meijer, E. W. *Angew. Chem., Int. Ed.* **2005**, *44*, 2275−2279.
(27) Wilson, A. J.; van Gestel, J.; Sijbesma, R. P.; Meijer, E. W. *Chem. Commun.* **2006**, 4404−4406.
(28) Palmans, A. R. A.; Vekemans, J. A. J. M.; Havinga, E. E.; Meijer, E. W. *Angew. Chem., Int. Ed.* **1997**, *36*, 2648−2651.
(29) van Gestel, J.; Palmans, A. R. A.; Titulaer, B.; Vekemans, J. A. J. M.; Meijer, E. W. *J. Am. Chem. Soc.* **2005**, *127*, 5490−5494.
(30) Nguyen, T. Q.; Martel, R.; Avouris, P.; Bushey, M. L.; Brus, L.; Nuckolls, C. *J. Am. Chem. Soc.* **2004**, *126*, 5234−5242.
(31) Bushey, M. L.; Nguyen, T.-Q.; Zhang, W.; Horoszewski, D.; Nuckolls, C. *Angew. Chem., Int. Ed.* **2004**, *43*, 5446−5453.
(32) Bushey, M. L.; Hwang, A.; Stephens, P. W.; Nuckolls, C. *Angew. Chem., Int. Ed.* **2002**, *41*, 2828−2831.
(33) Matsunaga, Y.; Nakayasu, Y.; Sakai, S.; Yonenaga, M. *Mol. Cryst. Liq. Cryst.* **1986**, *141*, 327−333.
(34) Matsunaga, Y.; Miyajima, N.; Nakayasu, Y.; Sakai, S.; Yonenaga, M. *Bull. Chem. Soc. Jpn.* **1988**, *61*, 207−210.
(35) Hanabusa, K.; Koto, C.; Kimura, M.; Shirai, H.; Kakehi, A. *Chem. Lett.* **1997**, 429−430.
(36) Shikata, T.; Ogata, D.; Hanabusa, K. *J. Phys. Chem. B* **2004**, *108*, 508−514.
(37) Sakamoto, A.; Ogata, D.; Shikata, T.; Urakawa, O.; Hanabusa, K. *Polymer* **2006**, *47*, 956−960.
(38) Ogata, D.; Shikata, T.; Hanabusa, K. *J. Phys. Chem. B* **2004**, *108*, 15503−15510.
(39) Blomenhofer, M.; Ganzleben, S.; Hanft, D.; Schmidt, H. W.; Kristiansen, M.; Smith, P.; Stoll, K.; Mader, D.; Hoffmann, K. *Macromolecules* **2005**, *38*, 3688−3695.
(40) Fontana, M.; Chanzy, H.; Caseri, W. R.; Smith, P.; Schenning, A. P. H. J.; Meijer, E. W.; Gröhn, F. *Chem. Mater.* **2002**, *14*, 1730−1735.
(41) Van der Schoot, P. In *Supramolecular Polymers*, 2nd ed.; Ciferri, A., Ed.; Taylor & Francis: London, 2005.
(42) Eliel, E. L.; Wilen, S. H.; Mander, L. N. *Stereochemistry of Organic Compounds*; Wiley-Interscience: Chichester, U.K., 1994.
(43) Shindo, Y.; Nishio, M. *Biopolymers* **1990**, *30*, 25−31.
(44) See Supporting Information.
(45) The fit function definition file for this equation, which can be imported in OriginPro (version 7.5 by OriginLab Cooperation), is available at our website: www.bmt.tue.nl/self-assembly.

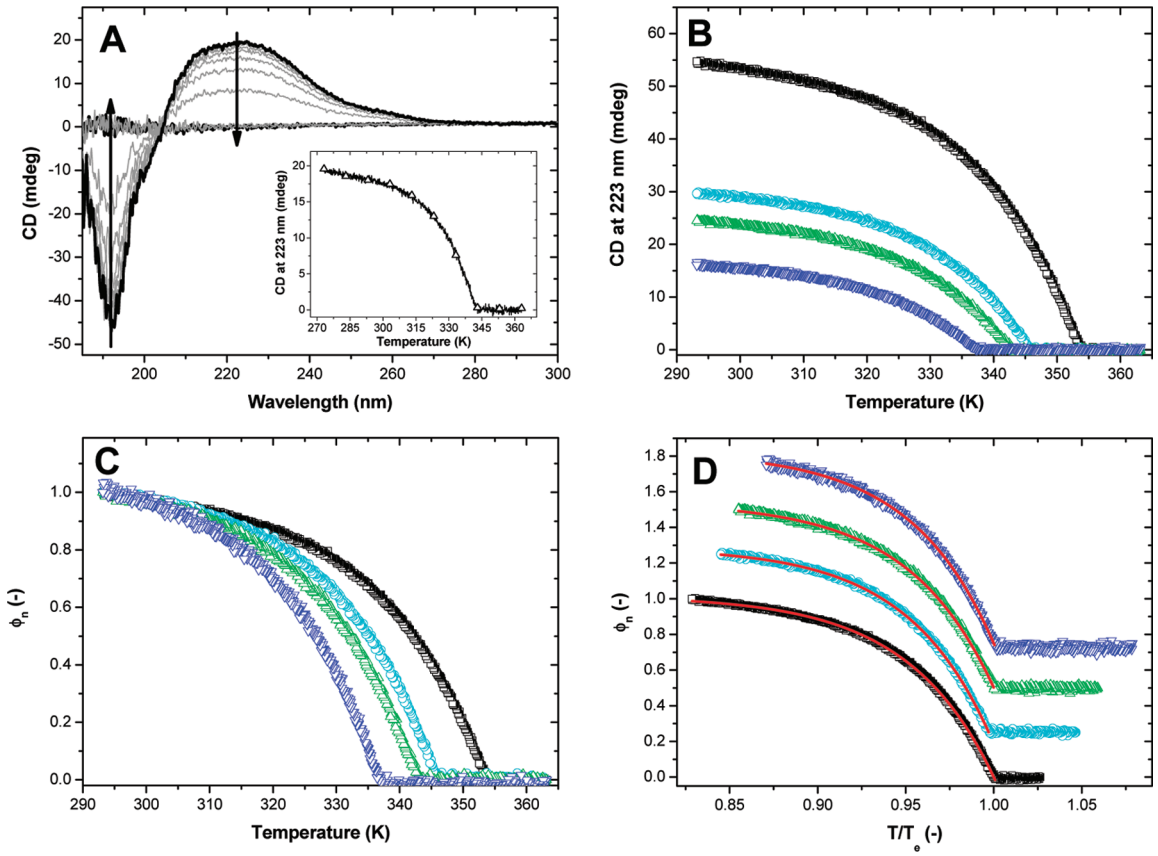

Figure 1. CD spectra of (*R*)-**1** in heptane (1.4×10^{-5} M) at temperatures between 20 and 90 °C with 10 °C intervals (arrow indicates increasing temperature). Inset shows the molar ellipticity at 223 nm as a function of temperature for the same solution (A). Molar ellipticity at 223 nm (B), normalized degree of aggregation (C), and degree of aggregation with fitted (red line) elongation regime using eq 2 (D) as a function of temperature for solutions of (*R*)-**1** in heptane, for different concentrations. In panel D the curves are shown with a 0.25 offset for each next concentration and as a function of the normalized temperature T/T_e. Concentrations: 3.8×10^{-5} M (black open square), 2.1×10^{-5} M (cyan open circle), 1.7×10^{-5} M (green open triangle pointing up), 1.2×10^{-5} M (blue open triangle pointing down).

where h_e is the molecular enthalpy release due to noncovalent interactions during elongation, T is the absolute temperature, T_e is the elongation temperature and R is the gas constant. ϕ_{SAT} is introduced as a parameter to ensure that ϕ_n/ϕ_{SAT} does not exceed unity.[46] At temperatures above the elongation temperature T_e (i.e., the nucleation regime) the fraction of aggregated molecules is described by[45]

$$\phi_n = K_a^{1/3} \exp\left[(2/3K_a^{-1/3} - 1)\frac{h_e}{RT_e^2}(T - T_e)\right] \qquad (2)$$

where K_a is the dimensionless equilibrium constant of the activation step at T_e.

The average length of the stack, $\langle N_n(T_e)\rangle$, averaged over the nucleated species, at the elongation temperature is given by

$$\langle N_n(T_e)\rangle = \frac{1}{K_a^{1/3}} \qquad (3)$$

Hence, a higher degree of cooperativity is expressed in a smaller K_a value and will lead to a larger nucleus before elongation sets in.

In the elongation regime the number-averaged degree of polymerization, averaged over all active species, $\langle N_n\rangle$, is given by

$$\langle N_n\rangle = \frac{1}{\sqrt{K_a}}\frac{\phi_n}{\phi_{SAT} - \phi_n} \qquad (4)$$

Using eq 1 the elongation regime of the normalized molar ellipticity data (i.e., for temperatures below T_e) could be fitted accurately using a simplified modeling procedure (Table 1, Figure 1C−D).[44] No deviations in the data from the model were observed at low temperatures, indicating that over the whole temperature range only linear, one-dimensional growth of the stacks has occurred. A decrease in T_e upon lowering the concentration of (*R*)-**1** was observed, and an enthalpy value of -60 kJ·mol^{-1} was determined which was independent of the concentration. Plotting the natural logarithm of the concentration versus the reciprocal T_e (Van't Hoff plot[44]) yielded an enthalpy of -66 kJ·mol^{-1} which is in good agreement with the value as derived from modeling the melting curves. A sharp transition in the molar ellipticity around T_e, was observed, indicative of a high degree of cooperativity in the self-assembly process. This high degree of cooperativity is also reflected in the small value of K_a, the equilibrium constant of the nucleation step, which was determined to be smaller than 10^{-6} (Table 1[44]). Using eq 3, the average stack length at T_e is at least 100 molecules,

(46) As the degree of normalization cannot exceed unity, ϕ_n/ϕ_{SAT} should be considered as the real degree of aggregation and ϕ_n could be regarded as the uncorrected degree of aggregation.

Table 1. Thermodynamic Parameters for the Self-Assembly of Solutions of Different Concentrations of (*R*)-**1** or **2** in Heptane, Determined by Modeling the Temperature-Dependent Spectroscopy Data

discotic	method	concentration (M)	ϕ_{SAT}	h_e (kJ·mol^{-1})	T_e (K)	K_a	$\langle N_n(T_e)\rangle$
(*R*)-**1**	CD	3.8×10^{-5}	1.018	−60.1	353.8	$\leq 10^{-6}$ [a]	≥100
		2.1×10^{-5}	1.039	−60.7	345.9	$\leq 10^{-6}$ [a]	≥100
		1.7×10^{-5}	1.043	−59.2	342.9	$\leq 10^{-6}$ [a]	≥100
		1.2×10^{-5}	1.077	−59.5	336.6	$\leq 10^{-6}$ [a]	≥100
	UV-vis	3.8×10^{-5}	1.026	−57.6	354.1	$\leq 10^{-6}$ [a]	≥100
		2.1×10^{-5}	1.047	−57.6	345.9	$\leq 10^{-6}$ [a]	≥100
		1.7×10^{-5}	1.053	−58.7	343.1	$\leq 10^{-6}$ [a]	≥100
		1.2×10^{-5}	1.074	−55.3	337.2	$\leq 10^{-6}$ [a]	≥100
2	UV-vis	4.2×10^{-5}	1.049	−66.7	361.8	1.6×10^{-4}	18
		3.5×10^{-5}	1.046	−69.6	356.5	1.1×10^{-4}	21
		2.2×10^{-5}	1.042	−69.9	350.0	0.9×10^{-4}	22
		1.8×10^{-5}	1.046	−69.8	346.3	0.6×10^{-4}	26

[a] No exact value for K_a could be determined because of its small value, which allowed us only to estimate an upper value.

suggesting that a relatively large nucleus needs to be formed before activation to a stable chiral stack will occur. The high cooperativity implies that, according to eq 4, the length of the stacks of (*R*)-**1** is over 10000 molecules at room temperature.[44]

Self-Assembly in Solution Followed by UV−Visible Spectroscopy. To study the self-assembly behavior of achiral discotic **2** and to compare this behavior with the self-assembly of chiral (*R*)-**1**, aggregation of (*R*)-**1** and **2** in dilute solution was further investigated with temperature-dependent UV−vis spectroscopy measurements in heptane (Figure 2A−B). For both compounds (*R*)-**1** and **2** at 90 °C (for concentrations between 1×10^{-5} and 5×10^{-5} M in heptane), an UV−vis absorption maximum was observed at 208 nm, which corresponds to the UV−vis absorption spectra in acetonitrile at room temperature in which (*R*)-**1** and **2** are molecularly dissolved species.[44] Upon cooling, a hypsochromic shift took place and the absorption maximum shifted to 193 nm, indicating the formation of a H-type of aggregates,[47] which is in agreement with the helical, columnar structure determined for a similar benzene-1,3,5-tricarboxamide by X-ray diffraction.[23]

We followed the self-assembly of (*R*)-**1** or **2** into aggregates, for different concentrations, by monitoring the UV−vis absorption at one wavelength as a function of temperature with a cooling rate of −1 K·min^{-1} (Figure 2C,D). The change in UV−vis absorption as a function of temperature for both (*R*)-**1** and **2** showed a similar transition as was observed for the temperature-dependent molar ellipticity of (*R*)-**1**, indicating that the self-assembly process of (*R*)-**1** and **2** could also be modeled by the nucleation−elongation self-assembly model. Normalizing the temperature-dependent UV−vis absorption data, allowed us to model the elongation regime of the self-assembly process (Figure 2E,F, Table 1). For discotic (*R*)-**1**, a value of −57 kJ·mol^{-1} was found for the enthalpy, h_e, which is in agreement with the value found based on the CD data. Furthermore, the T_e determined from the UV−vis data also corresponded with the value obtained from the CD data, revealing that both CD and UV−vis spectroscopy are probing the same self-assembly process in which (*R*)-**1** forms helical stacks without an intermediate nonhelical state. For discotic **2**, an enthalpy of −69 kJ·mol^{-1} was determined, which is close to the value of −75 kJ·mol^{-1} determined from the Van't Hoff plot.[44] Remarkably, these values are comparable to the earlier reported values for the structurally different oligo(*p*-phenylene vinylene) derivative (at 4.8×10^{-5} M, we found a T_e of 338 K and an h_e of −100 kJ·mol^{-1}).[20] For both (*R*)-**1** and **2** the enthalpy value was independent of concentration. The achiral discotic **2** was also found to aggregate at higher temperatures compared to its chiral analogue (*R*)-**1**, indicating that **2** forms more stable stacks, which is probably related to the branched side chains present in (*R*)-**1**. However, it should be noted that the difference is relatively small: at a concentration of $(1.7-1.8) \times 10^{-5}$ M, the T_e values are 343.1 and 346.3 K while the enthalpies are −58.7 and −69.8 kJ·mol^{-1} for (*R*)-**1** and **2**, respectively. This strongly suggests that **2** is also present in helical stacks, similar to (*R*)-**1**, only now in equal quantities of M and P helices, resulting in no net CD effect. For solutions of **2** at low temperatures, the UV−vis absorption started to show a small increase again, suggesting that a second process started to occur, which can probably be attributed to lateral aggregation (Figure 2D). This process is also visible in Figure 2F where at low temperatures the data started to deviate from the values predicted by the nucleation−elongation model. Also here no linear dichroism was observed.

A difference in the self-assembly behavior of (*R*)-**1** and **2** is also visible at temperatures close to T_e, in the region where nucleation takes place. For discotic **2**, the onset in the degree of aggregation, ϕ_n, around T_e, is more gradual compared to (*R*)-**1**, indicating a lower degree of cooperativity. Consequently, for **2** it was possible to model the nucleation regime around T_e with eq 2 to determine the equilibrium constant K_a.[44] The value for K_a was found to be dependent on the concentration; for the highest concentration (4.2×10^{-5} M) a value of 1.6×10^{-4} for K_a was determined, which decreased to 0.6×10^{-4} for the lowest concentration (1.8×10^{-5} M). At room temperature, stacks of **2** are shorter than stacks of (*R*)-**1** owing to the lower degree of cooperativity in the former case.[44] Based on eq 4, average stack lengths at room temperature of 10000 and 1000 are predicted for (*R*)-**1** and **2**, respectively. Currently we are determining the stack length and the size of the nucleus by small angle neutron scattering (SANS) and light scattering techniques.

These results show that although (*R*)-**1** and **2** are structurally very similar and they both self-assemble in a cooperative fashion, there is a considerable difference in the degree of cooperativity between the two discotics. The introduction of chirality in the molecules when going from achiral **2** to chiral (*R*)-**1** was found to have a significant effect in the self-assembly process of the discotics, as is reflected in the different K_a value, enthalpy value, and stability of the stacks for the two discotics.

The fact that these simple building blocks self-assemble via a cooperative mechanism suggests that this mechanism commonly operates in synthetic self-assembled systems. However, most self-assembled systems reported so far in literature, are described by an isodesmic model. We are currently investigating the mechanisms of other self-assembled systems developed in our group.

Mixed Systems. With our new understanding of the self-assembly process of the chiral and achiral discotics (*R*)-**1** and **2,** respectively, we further investigated mixed systems of (*R*)-**1** and **2** to understand the sergeants-and-soldiers principle that we have reported earlier.[21] Therefore solutions of sergeant (*R*)-**1** and soldier **2** in heptane, in which the fraction of (*R*)-**1** was

(47) Kasha, M.; Rawls, H. R.; El-Bayoumi, M. A. *Pure Appl. Chem.* **1965**, *11*, 371−392.

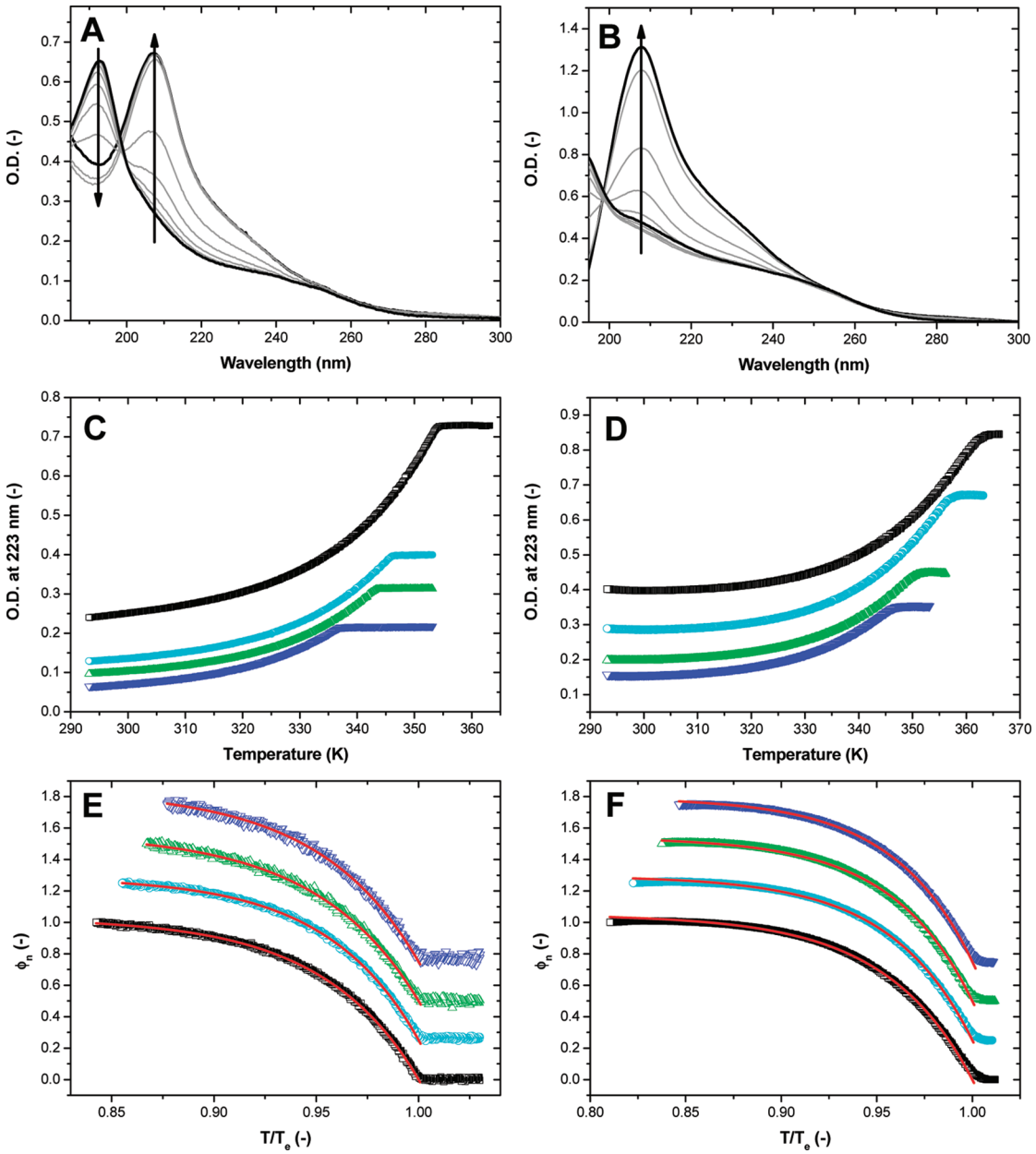

Figure 2. UV−vis absorption spectra of (*R*)-**1** in heptane (1.4×10^{-5} M, A) and **2** in heptane (3.5×10^{-5} M, B) at temperatures between 20 and 90 °C with 10 °C intervals (arrow indicates increasing temperature). UV−vis absorption at 223 nm[48] for (*R*)-**1** (C) and **2** (D) and degree of aggregation with fitted (red line) elongation regime using eq 2 for (*R*)-**1** (E) and **2** (F) as a function of temperature for solutions of (*R*)-**1** or **2** in heptane, for different concentrations. In panels E and F the curves are shown with a 0.25 offset for each next concentration as a function of the normalized temperature T/T_e. Concentrations for (*R*)-**1**: 3.8×10^{-5} M (black open square), 2.1×10^{-5} M (cyan open circle), 1.7×10^{-5} M (green open triangle pointing up), 1.2×10^{-5} M (blue open triangle pointing down). Concentrations for **2**: 4.2×10^{-5} M (black open square), 3.5×10^{-5} M (cyan open circle), 2.2×10^{-5} M (green open triangle pointing up), 1.8×10^{-5} M (blue open triangle pointing down).

changed while keeping the total concentration of (*R*)-**1** and **2** constant (2.1×10^{-5} M), were heated to 353 K to obtain the molecularly dissolved state. During the slow cooling of the mixtures, the UV−vis absorption and molar ellipticity were monitored. After addition of only 4% of sergeant (*R*)-**1** all columns had gained the same handedness as columns exclusively consisting of sergeant (*R*)-**1** (Figure 3A). This amplification of chirality is similar as reported earlier for this system.[21] With our new method we are now able to investigate in more detail the effects on mixing at the elongation temperature and cooperativity of the mixed systems. Although the maximum CD intensity is already reached after addition of 4% of sergeant, the enthalpy (h_e), elongation temperature (T_e) and the K_a value all depend linearly on the fraction of sergeant, at least in the regime where the CD intensity is saturated. (Figure 3A,B).[44]

These results reveal that during the self-assembly of mixtures of (*R*)-**1** and **2**, while cooling, no chiral amplification is observed in the thermodynamic parameters of the self-assembly. This suggests that the sergeant (*R*)-**1** is randomly incorporated in the growing stacks of **2** and vice versa, which is due to the similarity in structure and the relatively small differences in thermodynamic parameters of (*R*)-**1** and **2**.

To investigate also the kinetics involved in the sergeants-and-soldiers principle we added at room-temperature 100 μL

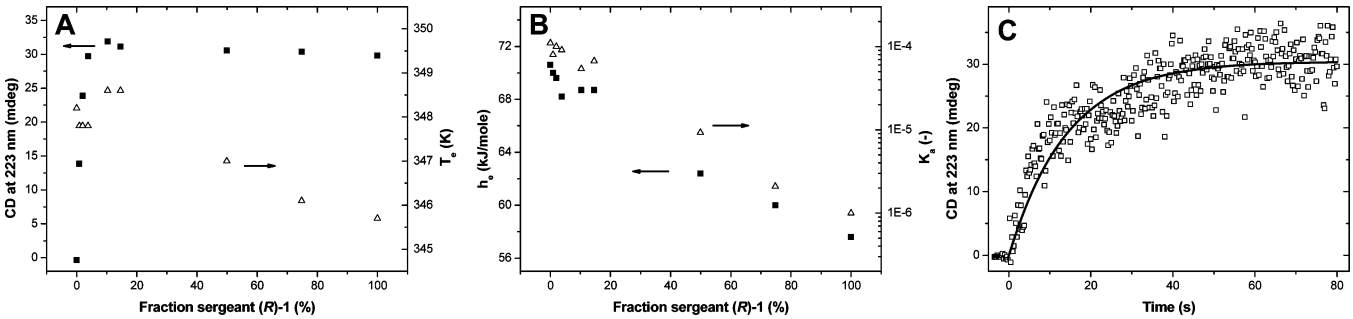

Figure 3. Molar ellipticity at 223 nm, elongation temperature, T_e (A), enthalpy release h_e and equilibrium constant K_a (B) for different sergeant/soldier mixtures. Molar ellipticity at 223 nm as a function of time, when at $t = 0$ 100 μL of a 2.1×10^{-5} M solution of sergeant (*R*)-**1** in heptane was added to 2.4 mL of a 2.1×10^{-5} M solution of soldier **2** in heptane (C).

of a 2.1×10^{-5} M solution of sergeant (*R*)-**1** in heptane to 2.4 mL of a 2.1×10^{-5} M solution of soldier **2** in heptane, while continuously monitoring the molar ellipticity. Remarkably, the molar ellipticity reached its final value in about 60 s, which was equal to the value observed previously for the 4/96 sergeant/soldier mixture. This fast exchange is in strong contrast with our oligo(*p*-phenylene vinylene) derivatives, in which the exchange rate was probed by energy transfer processes. In the latter case the exchange occurred on a time scale of days.[20,49,50]

At room-temperature both (*R*)-**1** and **2** are present in solution in long helical stacks. Apparently, at this temperature there is a rapid exchange of components between stacks of (*R*)-**1** and **2**. Also the interconversion, between M or P helicity in stacks of **2**, must be a fast process, to account for the observed rapid kinetics for the sergeant-and-soldiers principle. The exact mechanisms that describe the observed rapid kinetics on the one hand and the strong preference for one helicity in the presence of (*R*)-**1** on the other hand are part of ongoing research. Since the sergeants-and-soldiers principle can be considered as a two component system, these findings will have important consequences for the design of noncovalent routes toward self-assembled multicomponent objects.

Conclusion

We have described in this article the non-isodesmic, cooperative self-assembly of C_3-symmetrical discotic molecules (*R*)-**1** and **2**. With our nucleation−elongation model we were able to characterize all the thermodynamic parameters in the self-assembly process. The cooperative self-assembly mechanism observed for these simple and widely studied building blocks suggests that this mechanism operates more commonly in synthetic self-assembled systems. Currently we are studying other self-assembled systems by temperature-dependent optical measurements to get insight in why some systems self-assemble via an isodesmic model and others via a cooperative model. Furthermore, we are characterizing the stages in the self-assembly process by complementary techniques, such as SANS and light scattering.

With the nucleation−elongation model we also could investigate the sergeants-and-soldiers principle that has been reported for (*R*)-**1** and **2**. Our observation that the sergeants-and-soldiers principle is a rapid process has important consequences for the design of noncovalent routes toward self-assembled multicomponent objects. In addition it illustrates that sergeant-and-soldiers experiments are a nice tool to investigate the dynamics in self-assembled systems.

Acknowledgment. We thank J. J. van Gorp and J. R. Roosma for their part in the synthesis. P. van der Schoot is acknowledged for stimulating discussions. The authors thank the NRSC-Catalysis for funding.

Supporting Information Available: Experimental conditions, details about the nucleation−elongation model, modeling procedures and supporting figures and tables. This material is available free of charge via the Internet at http://pubs.acs.org.

JA075987K

(48) The UV-vis absorption was monitored at 223 nm and not at 208 nm (wavelength corresponding to the maximum absorption) because less background absorption by the solvent is present at this higher wavelength, which resulted in a better signal-to-noise ratio. Monitoring at either wavelength resulted in an identical transition, after normalization. The temperature-dependent UV-vis absorption data were corrected for this solvent absorption. For more details, see Supporting Information.

(49) Hoeben, F. J. M.; Herz, L. M.; Daniel, C.; Jonkheijm, P.; Schenning, A. P. H. J.; Silva, C.; Meskers, S. C. J.; Beljonne, D.; Phillips, R. T.; Friend, R. H.; Meijer, E. W. *Angew. Chem., Int. Ed.* **2004**, *43*, 1976−1979.

(50) Hoeben, F. J. M.; Shklyarevskiy, I. O.; Pouderoijen, M. J.; Engelkamp, H.; Schenning, A. P. H. J.; Christianen, P. C. M.; Maan, J. C.; Meijer, E. W. *Angew. Chem., Int. Ed.* **2006**, *45*, 1232−1236.